中國機械工程學刊第四十一卷第一期第 21~28 頁(民國一百零九年)
Journal of the Chinese Society of Mechanical Engineers, Vol.41, No.1, pp 21~28 (2020)

Effects of Coatings Thickness on the Structural and Mechanical Performances of High Entropy Alloy Nitride Films

Zhi-Wei Liu*, Ching-Been Yang**, Chih-Chung Hu***, Jun-Cheng Lin****, Chung-Chen Tsao****and Chun-Yao Hsu****

Keywords：high entropy alloys, film thickness, cutting performance, nano-indentation, direct current magnetron sputtering

ABSTRACT

Multi-element high-entropy alloys systems (more than five elements) are alloy with X (5 < X < 13) principal elements each possess an atomic percentage no more than 35%. This paper determines the coating thickness for the high-entropy alloy (HEAs) nitride films using reactive direct current magnetron sputtering, that are deposited on ceramic insert tools and glass substrates. Using equimolar AlCrNbSiTiV HEA target and Ar plasma and N_2 reactive gases. The coated nitride films are characterized using scanning electron microscopy (SEM), energy dispersive X-ray analysis (EDS), transmission electron microscopy (TEM) and a nano-indentation technique. The TEM patterns show that the (AlCrNbSiTiV) N films have a simple face-center-cubic (FCC) structure. The (AlCrNbSiTiV) N films are homogeneous, very compact and adhere perfectly to the substrate. The films are uniform and dense, adhere perfectly to the substrate, the results of the Rockwell indentation test are categorized as HF1. The experimental results show that after cutting, the coated tool has a minimum flank wear of 16.91 μm and a surface roughness Ra of 3.79 μm for a sputtering time of 25 min and a film thickness of 431 nm. When the coating thickness exceeds 431nm the elastic recovery and the hardness of the (AlCrNbSiTiV) N film increases However, further increases in the coating thickness results in a decrease in the cutting qualities.

Paper Received September, 2019. Revised October, 2019. Accepted October, 2019.Author for Correspondence: Chung-Chen Tsao and Chun-Yao Hsu

* *Lecturer, Department of Mechanical and Electrical Engineering, Dongguan Polytechnic, Dongguan 523808, China*

** *Professor, Department of Mechanical Engineering, Nanya Institute of Technology, Taoyuan, Taiwan*

*** *Assistant Professor, Department of Mechanical Engineering, Ming Chi University of Technology, Taipei, Taiwan*

**** *Professor,* Department of Mechanical Engineering, Lunghwa University of Science and Technology, Taoyuan, *Taiwan*

INTRODUCTION

Transition metal nitride and carbide films that are synthesized by physical vapor deposition or chemical vapor deposition have been extensively studied. Sputtering technology (ST) is used to improve or modify the mechanical properties and surface quality of tools, parts and structures to save on manufacturing costs and are the subject of many studies. Solid ceramic nitride hard coatings, such as TiN, CrWN, TiAlN and CrAlSiN, find various industrial applications because of their high hardness, excellent wear resistance and high thermal and chemical stability. Chen et al. (2016) showed that the surface roughness of a workpiece and the flank wear are significantly reduced for tool that is coated with CrAlSiN hard films using direct current (DC) reactive magnetron co-sputtering. It is found that the optimized CrAlSiN hard films deposition conditions, the hardness, Young's modulus and friction coefficient were 31.26 GPa, 258.58 GPa and 0.50, respectively. Hsieh et al. (2017) reported the effect of transition metal nitride (ZrN, WN and ZrWN) films on the mechanical performance and cutting tool properties. Cutting of AISI 316 stainless steel was studied with and without CrWN films coated tools, which show that use of a CrWN films coated tool remarkably decreases surface roughness and flank wear. Wu et al. (2019) The study shows that samples that are coated with ternary nitride (ZrWN) perform better than samples that are coated with binary nitride (ZrN and WN). A comparison of the experimental results shows that samples coated with ZrWN give a better cutting property and have better mechanical characteristic than samples coated with ZrN and WN.

Traditional metallic alloys use one or two main elements in the primary phase and minor alloys elements are added to improve the material properties (Li et al. 2016). However, high entropy alloys (HEAs), which represent a new concept in metallic materials, are not like metallic alloys (Tsai et al. 2014). In general, HEAs contain at least five principal elements in equimolar or near-equimolar concentrations: the concentration of each element is between 5% and 35%. Huang et al. (2009) noted that HEA nitride films have a characteristic of FCC phase structure. After interrupted turning, tools that are coated with a HEA nitride film have a much longer tool life than uncoated tools. The correlation of the results with structure analysis and tool life shows that using high power impulse magnetron sputtering discharge produce higher (AlCrNbSiTiV) N film density, a smoother surface structure and a higher hardness surface (Chang et al. 2018). Wan et al. (2018) deposited HEA nitride film onto a cutter insert using reactive DC magnetron sputtering with an equimolar HEA target. The study determined the effect of a negative substrate bias on the structure, the hardness, the elastic recovery and the performance of the cutting tool. The machined surface for a coated tool for which the substrate bias is –100 V exhibits fewer surface defects, such as pockmarks or cracks. Chang et al. (2018) reported the influence of the nitrogen flow ratio (from 0 to 40%) on the chemical composition, structure, mechanical characteristics and cutting tool properties of the (AlCrNbSiTiV) N film. The machining surface of a coated tool shows fewer surface defects and the tool flank wear is decreased. The ions are highly energetic ions so the films deposited using HIPIMS are smoother, denser and better crystallized. Hsieh et al. (2018) deposited a HEA nitride film using reactive DC magnetron sputtering with an equimolar HEA target. The TEM patterns confirm that the HEA nitride films have a simple FCC structure. The HEA nitride film coatings are homogeneous, adhere perfectly to the substrate and exhibit good tribological characteristics. Experimental results show that a (AlCrNbSiTiV) N film coating significantly enhanced the mechanical characteristics. Other studies show that the substrate temperature (Erdoğan et al. 2019; Amroun et al. 2019), the sputtering time (Astinchap et al. 2019; Ge et al. 2019), the substrate negative bias (Deng et al. 2019; Liu et al. 2017) and the ratio of the nitrogen to argon gas flow (Peyqambarian et al. 2019; Pamuk et al. 2018) have a significant effect on the characteristics of coated objects. Using the sputtering conditions mentioned previously, this study determines the effect of (AlCrNbSiTiV) N coatings of different thickness on the structural and mechanical performance.

EXPERIMENTAL METHOD

This experiment uses anti-oxidation elements (Al, Cr, and Si), lubricating elements (V) and high solid solution strengthening elements (Ti, Nb) to form a (AlCrNbSiTiV) HEA system. The (AlCrNbSiTiV) N films were deposited on discarded ceramic insert tools (TNMG160404R-UMT1200A) and glass, in order to determine the effect on the mechanical properties and dry cutting quality of substrate temperature, sputtering time, substrate bias and the nitrogen to argon ratio, as shown in Table 1.

Table 1. The various deposition parameters and the levels

Deposited parameter	Level 1	Level 2	Level 3	Level 4	Level 5
Substrate temperature (ºC)	25	100	200	300	400
Sputtering time (min)	15	25	35	45	55
substrate bias (V)	0	–50	–100	–150	–200
$N_2/(N_2 + Ar)$ ratio (%)	0	10	20	30	40

The effect of sputtering time (15, 25, 35, 45, 55 min) on a (AlCrNbSiTiV) N film that is growth using a DC power of 180 W, a substrate bias of –100 V, a substrate temperature of 100ºC, a chamber pressure of 1×10^{-2} torr and a nitrogen to argon ratio of 20% is shown in Table 2. The sputtering and reactive gases are Ar (purity: 99.995%) and N_2 (purity: 99.995%), respectively. The respective diameter and thickness of HEA (AlCrNbSiTiV) target are about 50 mm and 6 mm. The substrates were ceramic insert cutting tools and soda-lime glass, which were ultrasonically cleaned in isopropyl alcohol (IPA) for 15 min, rinsed with de-ionized water and dried in nitrogen. The target was pre-sputtered for 10 min to remove any contamination.

Table 2. Deposition parameters for the (AlCrNbSiTiV) N film

Substrate	Soda-lime glass and discarded ceramic insert tools (TNMG160404R--UMT1200A)
Working pressure	1×10^{-2} torr
Base pressure	5×10^{-6} torr
Substrate-to-target distance	85 mm
Target diameter/thickness	50 mm/6 mm
Substrate rotate speed	50 rpm
DC power	180 W

The magnetron sputtering system is microprocessor controlled. The effect of different coating thicknesses on the surface microstructure and the mechanical properties of the (AlCrNbSiTiV) N coatings when they are used for turning S45C were determined. A micro-shape analyzer (α-step, KOSAKA, ET-4000A) was used to determine the surface morphology and the thickness and deposition rate for the (AlCrNbSiTiV) N coatings. A field emission scanning electron microscope (FESEM, JEOL JSM-6500F) was used to observe the surface morphology and the cross-section of the coatings. The composition ratio of the coatings was determined using Energy-dispersive X-ray spectroscopy (EDS). XRD (Rigaku 2200 X-ray generator) with a θ~2θ configuration was used to generate Cu K_{α} radiation (λ=1.54056 Å), using an electron-excited copper target as an incident light source to obtain an XRD diffraction pattern. Microstructural observations used an analytical transmission electron microscopy system (Philips Tecnai F20 G2 FEI-TEM). The JCPDS card was used to determine the type and crystal structure of the (AlCrNbSiTiV) coatings. The coefficient of friction was measured using a Ball-on-disk Tribometer (CSM Instruments, Switzerland). The (AlCrNbSiTiV) coatings that were deposited on glass using a 6.0 mm diameter Al_2O_3 ball, tangential speed of 10 cm/s and a sliding distance of 30 m under a load of 1 N. After the test, the wear depth for the test specimen was measured using a micro-shape analyzer (α-step). The film hardness was measured using a dynamic micro hardness tester (Fischer, HM-2000).

A series of turning experiments for S45C (Φ40mm×400mm) used a cutting velocity of 200 m/min, a 0.2 mm/rev feed rate, a 2 mm depth of cut and a 300 mm cutting length, using a CNC lathe (LEADWELL T-6). For dry cutting, instead of using coolant, nonpollutant machining processes with coated tool inserts will improve cost effectiveness and reduce pollution in the environment. All experiments were performed three times using no coolant. After turning, the flank wear was measured using a tool microscope (Micro Vu, Vertex 220). A surface roughness instrument (Mitutoyo, SJ-410) was used to measure the surface roughness of the turned S45.

RESULTS AND DISCUSSIONS

Table 3 shows the film thickness, the flank wear and the surface roughness for different sputtering times. The deposition rate ranges from 17.28 to 18.85 nm/min, the value for film thickness ranges from 261.5 to 979.6 nm. It is seen that the deposition rate has little change with different sputtering times. The results in Table 3 show that after dry turning S45C, the coated tool has the lowest deposition rate (17.28 nm/min), a minimum flank wear of 16.91 μm and the least surface roughness Ra of 3.79 μm for a sputtering time of 25 min and a film thickness of 431 nm. The flank wear and the surface roughness for a coated tool that is sputtered for 25 min show a respective improvement of 31.42% and 6.05%. When the thickness of the (AlCrNbSiTiV) N film coating exceeds 431 nm, the flank wear and the surface roughness increase. However, further increases in the coating thickness results in a decrease in cutting qualities. After dry cutting with an (AlCrNbSiTiV) N film coated tool inserts, we achieved much longer tool life than that uncoated tools. Fig. 1 shows the SEM images for the surface roughness (left) and flank wear (right) with a (AlCrNbSiTiV) N film coating at different sputtering times: (a, b) 15 min, (c, d) 25 min, (e, f) 35 min, (g, h) 45 min and (i, j) 55 min.

Table 3. The film thickness, flank wear and surface roughness for different sputtering times

Sputtering time (min)	Film thickness (nm)	Deposition rate (nm/min)	Flank wear (μm)	Surface roughness Ra (μm)
uncoated	0	0	24.66	4.05
15	261.5	17.43	17.931	3.87
25	**431.9**	**17.28**	**16.91**	**3.79**
35	613.9	17.54	17.64	3.90
45	803.5	17.85	17.65	3.92
55	979.6	17.81	17.35	3.79

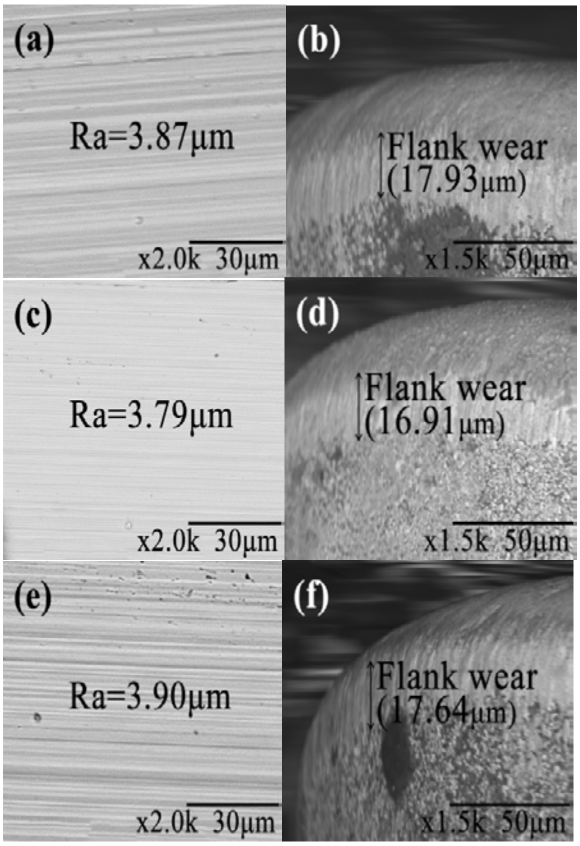

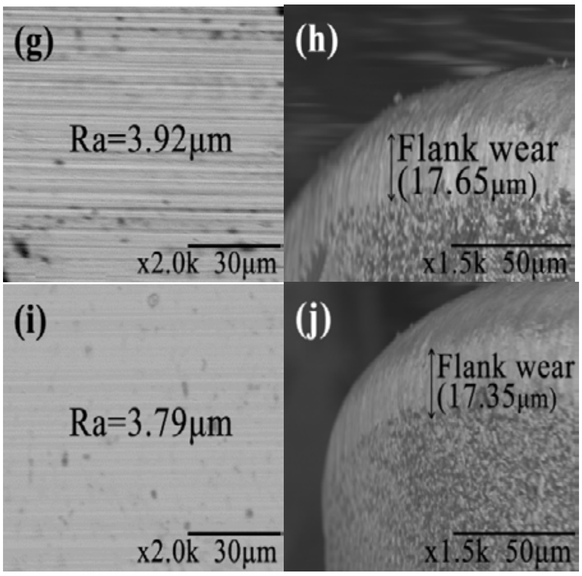

Fig. 1. SEM images showing the surface roughness (left) and flank wear (right) with a (AlCrNbSiTiV) N film coating at different sputtering times: (a, b) 15 min, (c, d) 25 min, (e, f) 35 min, (g, h) 45 min and (i, j) 55 min.

Fig. 2 shows the cross section and surface morphology of(AlCrNbSiTiV) N films with different sputtering times. The shorter the sputtering time is, the thinner the film thickness. It is seen that the (AlCrNbSiTiV) N films are homogeneous, very compact and adhere perfectly to the substrate. No cracking or peel-off is examined after coatings. In some regions of the (AlCrNbSiTiV) N film, a growth morphology in the form of columnar structure. The surface of the coating exhibits a grain like structure. Fig. 3 shows the EDS composition of(AlCrNbSiTiV) N films with different sputtering times. The experimental results show that the influence of EDS composition for (AlCrNbSiTiV) N film is not significant to change the sputtering time. However, the nitride has the largest concentration (at. %) in the overall(AlCrNbSiTiV) N film compositions.

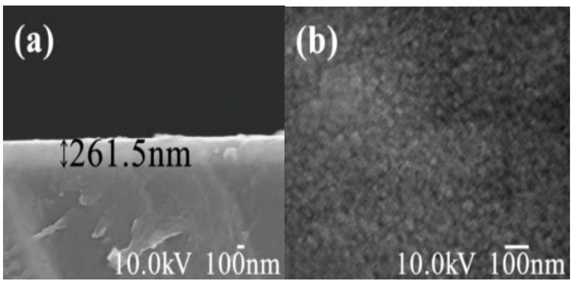

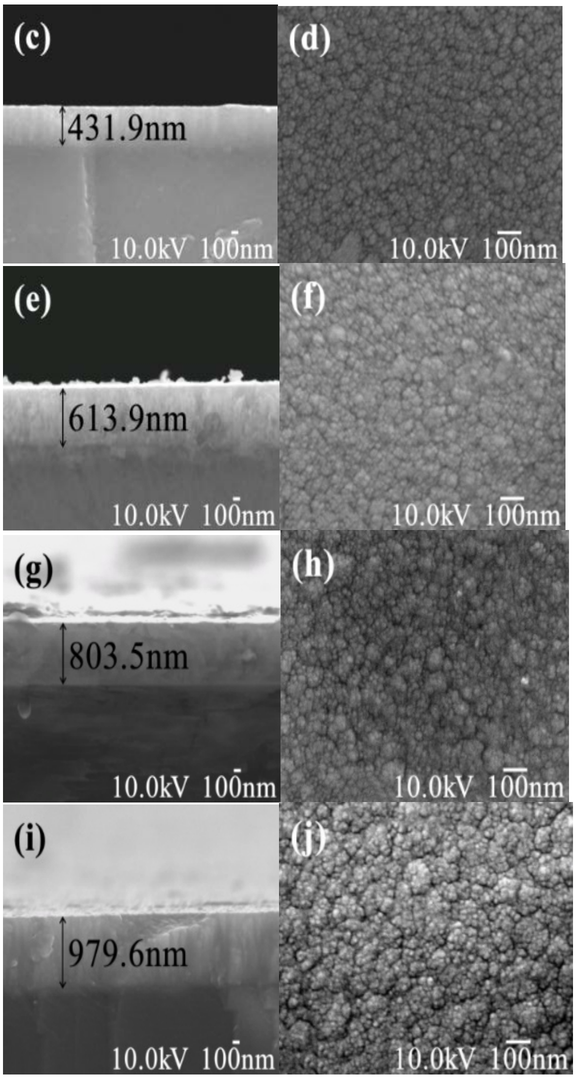

Fig. 2. The cross section and surface morphology of (AlCrNbSiTiV) N films that are sputtered for: (a, b) 15 min, (c, d) 25 min, (e, f) 35 min, (g, h) 45 min and (i, j) 55 min.

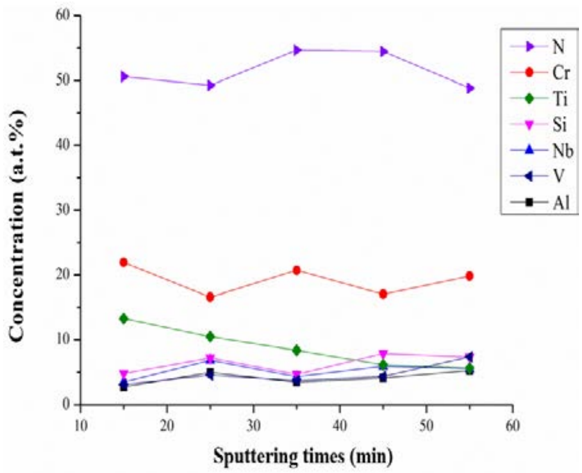

Fig. 3. The EDS composition of (AlCrNbSiTiV) N films for different sputtering times.

Fig. 4 (a) shows the bright-field TEM micrographs and Fig. 4 (b) shows the corresponding selected area electron diffraction (SAED) pattern for the HEA (AlCrNbSiTiV) N films. As can be seen, this film shows a typical columnar microstructure, and composed of a series of concentric circular diffraction rings, which shows a simple face-center-cubic (FCC) crystal phase. These results are similar to those of Chang et al. (2018) Due to stress relaxation away from the interface between the HEAs nitride films and the substrate, the lattice begins to form nanograins and the columnar structure of the FCC is developed (Liang et al. 2016).

Fig. 5 shows the hardness of (AlCrNbSiTiV) N film with different sputtering times. The hardness ranges from 604.2 to 807.3 Hv. It can be seen from Fig. 5 that the maximum hardness generated is 807.3 Hv at sputtering time of 25 min. Fig. 6 shows the correlation between friction coefficient and wear distance for (AlCrNbSiTiV) N films with different sputtering times. It can be seen from Fig. 6 that the minimum friction coefficient is 0.78 at sputtering time of 25 min.

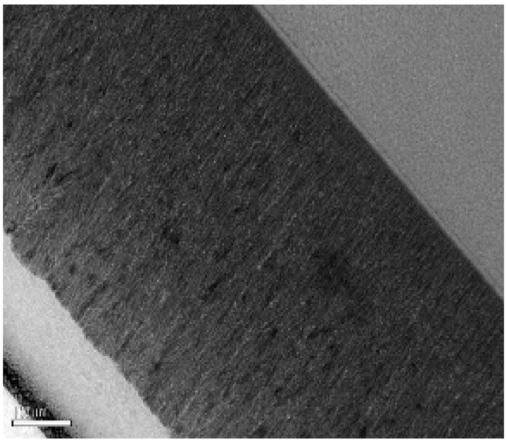

(a)

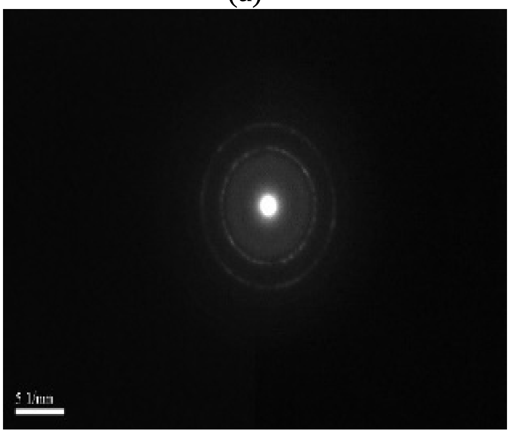

(b)

Fig. 4. (a) TEM image and (b) the selected area electron diffraction pattern for the HEA (AlCrNbSiTiV) N films.

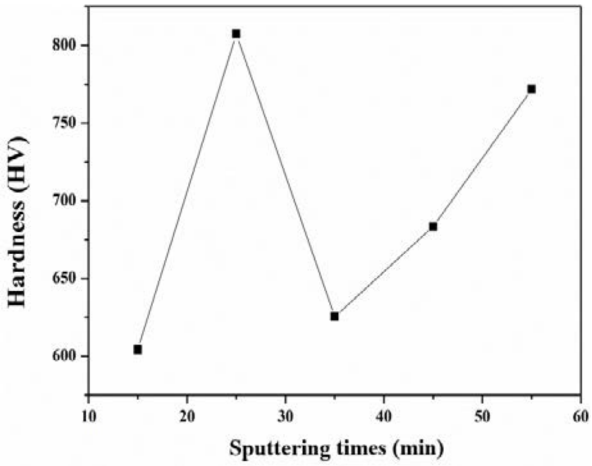

Fig. 5. The hardness of (AlCrNbSiTiV) N film for different sputtering times.

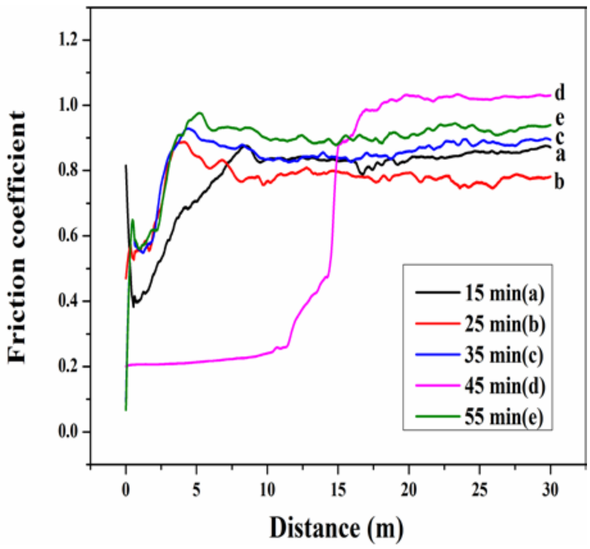

Fig. 6. The correlation between the coefficient of friction and the wear distance for (AlCrNbSiTiV) N films for different sputtering times.

A Rockwell C indentation test (maximum applied force 1471 N) was used to determine the adhesive strength of the coatings. An Indentec hardness tester was used to determine the Rockwell-C adhesion. For the adhesion analysis techniques reported by Yang et al. (2015) defined six classes (HF1–HF6) of indentation that qualitatively estimate the adhesion of thin films to their substrates. Fig. 7 shows the indented contours of the coated samples. The indentation is smooth and some radial cracks originate from the center. The (AlCrNbSiTiV) N films that are produced by this study are classified as HF1, which represents good adhesive strength.

Nano-indentation is used to study the nanomechanical performance of these thin films. The hardness (GPa), the elastic modulus (GPa) and the elastic recovery (%) are measured by means of the load-displacement curve and the film's wear resistance. The nanomechanical performance of the films are measured in terms of indentor penetration depth at maximum load (*h*max), the depth of the residual indent (*hr*), and the elastic recovery (Re).

Fig. 8 shows the nano-indentation load-displacement curves for (AlCrNbSiTiV) N films under different sputtering times. All of the curves show consecutive loading and unloading processes. It can be seen from Fig. 8 that the magnitude relationships of load/sputtering time for (AlCrNbSiTiV) N films in order are 7.7 mN/55 min, 7.6 mN/25 min, 6.7 mN/ 45min, 6.7 mN/35 min and 6.5 mN/15 min, respectively. With different maximum loads (6.5, 7.6, 6.7, 6.7 and 7.7 mN), the depths of indentor penetration (*h*max) are 204.27, 207.13, 206.36, 206.48 and 206.48 nm. The depths of the residual indent (*hr*) are 107.11, 108.04, 125.01, 122.16 and 122.16 nm, and obtained the elastic recovery $(h\max - hr)/h\max \times 100\%$ (Re) are 47.56, 47.84, 39.42, 40.83 and 40.83%. As a result for using sputtering times of 25 min, shows the high hardness of 807.3 Hv from Fig. 5 and elastic recovery of 47.84%.

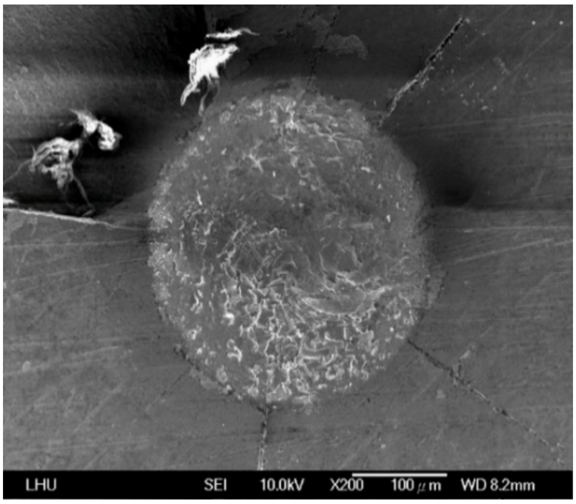

Fig. 7 Fracture morphology for samples that are coated with a (AlCrNbSiTiV) N film, measured using a Rockwell-C hardness tester.

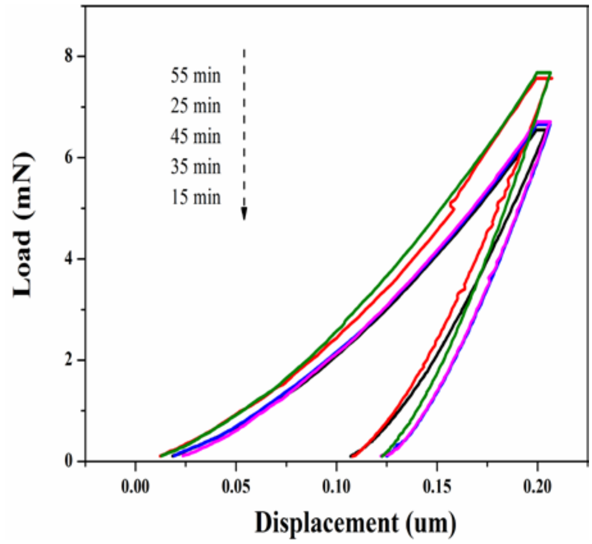

Fig. 8. The nano-indentation load-displacement curves for (AlCrNbSiTiV) N films under different sputtering times from 15 to 55 min.

CONCLUSIONS

This study determines the effect of (AlCrNbSiTiV) N coatings of different thickness on the structural, mechanical property and dry cutting performance. The important results are summarized as follows:

1. The dry cutting result shows that a sputtering time of 25 min gives a minimum flank wear of 16.91 μm and a surface roughness Ra of 3.79 μm. The rate of flank wear and surface roughness are respectively reduced by 31.42% and 6.05%, compared with the figures for an uncoated tool.
2. The deposition rate of (AlCrNbSiTiV) N films has little change with different sputtering times.
3. Nitride has the largest concentration (at.%) in the overall (AlCrNbSiTiV) N film composition.
4. TEM micrographs for the HEA (AlCrNbSiTiV) N films, which shows a simple face-center-cubic (FCC) crystal phase structure.
5. For a sputtering time of 25 min, the hardness of (AlCrNbSiTiV) N films has a maximum value and the coefficient of friction has a minimum value.
6. As a result for using sputtering times of 25 min, shows the elastic recovery of 47.84%.

ACKNOWLEDGMENT

This research is partially supported by Ministry of Science and Technology, Taiwan, ROC, under contract MOST-107-2622-E-262-004-CC3 and MOST 108-2622-E-262-007-CC3**.**

REFERENCES

Amroun, M.N. and Khadraoui, M., “Effect of substrate temperature on the properties of SnS_2 thin films”, *Optik*, Vol. 184, pp. 16-27 (2019).

Astinchap, B., “Fractal and statistical characterization of Ti thin films deposited by RF-magnetron sputtering: The effects of deposition time”, *Optik*, Vol. 178, pp. 231-242 (2019).

Chang, K.S., Chen, K.T., Hsu, C.Y. and Hong, P.D., “Growth (AlCrNbSiTiV) N thin films on the interrupted turning and properties using DCMS and HIPIMS system”, *Applied Surface Science*, Vol. 440, pp. 1-7 (2018).

Chang, C.H., Yang, C.B., Sung, C.C. and Hsu, C.Y. “Structure and tribological behavior of (AlCrNbSiTiV) N film deposited using direct current magnetron sputtering and high power impulse magnetron Sputtering”, *Thin Solid Films*, Vol. 668, pp. 63-68, (2018).

Chen, D.Y., Tsai, C.H., Yang, W.J., Liu, D.W. and Hsu, C.Y., “Reactive co-sputter deposition and properties of CrAlSiN hard films for enhancement of cutting tools”, *International Journal of Refractory Metals and Hard Materials*, Vol. 58, pp. 110-116 (2016).

Deng, Q.Y., Wang, C.M., Zhang, T.F., Yang, W.M. and Leng, Y.X., “Regulating the uniformity of DLC films in ECR plasma with negative substrate biasing”, *Surface and Coatings Technology*, Vol. 365, pp. 15-23 (2019).

Erdoğan, E. and Kundakçı, M., “Influence of substrate and substrate temperature on the structural, optical and surface properties of InGaN thin films prepared by RFMS method”, *Microelectronic Engineering*, Vol. 207, pp. 15-18 (2019).

Ge, S.W., Zhang, B.H. and Yang, C.T., “Characterization of Er-doped AlN films prepared by RF magnetron sputtering”, *Surface and Coatings Technology*, Vol. 358, pp. 404-408 (2019).

Hsieh, T.H., Zhu, Y.J., Yu, Z.H., Tang, C.Y., Hsu, C.H. and Hsu C.Y., “Mechanical and Tribological Properties of CrWN Nanostructured Hard Films”, *Journal of nanoscience and nanotechnology*, Vol. 17, pp. 5031-5036 (2017).

Hsieh, T.H., Hsu, C.H., Wu, C.Y., Kao, J.Y. and Hsu, C.Y., “Effects of deposition parameters on the structure and mechanical properties of high-entropy alloy nitride films”, *Current Applied Physics*, Vol. 18, pp. 512-518 (2018).

Huang, P.K. Yeh, J.W. “Effects of nitrogen content on structure and mechanical properties of multi-element (AlCrNbSiTiV) N coating”, *Surface & Coatings Technology*, Vol. 203, pp. 1891-1896 (2009).

Li, D.Y. and Zhang, Y., “The ultrahigh charpy impact toughness of forged $Al_xCoCrFeNi$ high entropy alloys at room and cryogenic temperatures”, *Intermetallics*, Vol. 70, pp. 24-28 **(**2016**)**.

Liang, S.C., Chang, Z.C., Tsai, D.C., Lin, Y.C., Sung, H.S., Deng, M.J. and Shieu, F.S., “Effects of substrate temperature on the structure and mechanical properties of (TiVCrZrHf) N coatings”, *Applied Surface Science*, Vol. 257, pp. 7709-7713 (2011).

Liu, J., Liu, B., Zhang, X.S., Guo, X.J. and Liu, S.Z., “Improvement of crystallinity for poly-Si thin film by negative substrate bias at low temperature”, *Thin Solid Films*, Vol. 629, pp. 1891-1896 (2017).

Pamuk, S. and Sojiphan, K., “Effects of argon-nitrogen backing gas ratios on microstructure and corrosion resistance of duplex stainless steel pipe ASTM A790 welds by gas tungsten arc welding process”, *Materials Today: Proceedings*, Vol. 5, No. 3, pp. 9512-9518 (2018).

Peyqambarian, M., Azadi, M. and Ahangarani, S. “An evaluation of the effects of the N_2/Ar gas flux ratio on various characteristics of TiC0.3N0.7 nano-structure coatings on the cold work tool steel by pulsed DC-PACVD”, *Surface and Coatings Technology*, Vol. 366, pp. 366-374 (2019).

Tsai, M.H. and Yeh, J.W., “High-Entropy Alloys: A Critical Review”, *Material Research Letters*, Vol. 30, pp. 107-123 (2014).

Wan, S.F., Zuo, D.L., Hsiao, R.C., Kao, J.Y., Yu, Z.H. and Hsu, C.Y., “Structure and mechanical properties of (AlCrNbSiTiV) N thin films deposited using reactive direct current magnetron sputtering”, *science of Advanced Materials*, Vol. 10, pp. 1230-1235 (2017).

Wu, C.Y., Chen, J.H., Kuo, C.G., Twu, M.J., Peng, S.W. and Hsu, C.Y., “Effect of deposition parameters on the structure and properties of ZrN, WN and ZrWN films”, *Bulletin of Materials Science*, Vol. 42, pp. 38-45 (2019).

Yang, K., Xian, G., Zhao, H., Fan, H. J., Wang, H. and Wang, “Du, H., Effect of Mo content on the structure and mechanical properties of (TiAlMo)

N films deposited on WC–Co cemented carbide substrate by magnetron sputtering", *International Journal of Refractory Metals and Hard Materials*, Vol. 52, pp. 29-35 (2015).

鍍層厚度對高熵合金氮化薄膜微結構和機械性質的影響

劉志偉
東莞職業技術學院機電工程學院

楊慶彬
南亞技術學院機械工程系

胡志中
明志科技大學機械工程系

林鈞晟 曹中丞 許春耀
龍華科技大學機械工程系

摘 要

本文採用反應性直流磁控濺鍍，製備高熵合金氮化物薄膜於於瓷金刀具，不銹鋼及玻璃基材。等莫爾 AlCrNbSiTiV 高熵合金靶材，Ar 等電漿氣體，N_2 反應氣體，探討不同高熵合金氮化物薄膜厚度(改變沉積時間)，對薄膜微結構，機械性質及鍍層刀具切削行為的影響。氮化物薄膜應用掃描電子顯微鏡(SEM)，能量色散 X 射線分析(EDS)，穿透式電子顯微鏡(TEM)和奈米壓痕技術進行表徵分析。由 TEM 圖顯示，(AlCrNbSiTiV) N 薄膜具有簡單的面心立方(FCC)結構。研究結果顯示，薄膜均勻且緻密，完美地粘附在基材表面。經洛氏壓痕測試，結果顯示氮化物薄膜為 HF1 優良等級附著性。鍍層刀具切削加工實驗結果顯示，薄膜沉積時間 25 分鐘(薄膜厚度為 431 nm)，有最小的刀腹磨損量 16.91 μm，切削加工件表面粗糙度(Ra)為 3.79 μm。當鍍層厚度高於 431 nm 時，(AlCrNbSiTiV) N 薄膜的彈性恢復量及薄膜硬度有增大的趨勢，但是當鍍層厚度進一步增加，會降低切削加工品質。